UCRL 9886

UNIVERSITY OF CALIFORNIA

Ernest O. Lawrence

Radiation Laboratory

THE PION-PION CROSS SECTION BY THE CHEW-LOW METHOD

BERKELEY, CALIFORNIA

UCRL-9886
UC-34 Physics
TID-4500(16th Ed.)

UNIVERSITY OF CALIFORNIA
Lawrence Radiation Laboratory
Berkeley, California

Contract No. W-7405-eng-48

THE PION-PION CROSS SECTION BY THE CHEW-LOW METHOD

D. Duane Carmony

Thesis

October 1961

Printed in USA. Price $1.00. Available from the
Office of Technical Services
U. S. Department of Commerce
Washington 25, D.C.

THE PION-PION CROSS SECTION BY THE CHEW-LOW METHOD

Contents

UCRL-9886
UC-34 Physics
March 2, 1962

UNIVERSITY OF CALIFORNIA

Lawrence Radiation Laboratory
Berkeley, California

Contract No. W-7405-eng-48

ERRATA

TO: Recipients of UCRL-9886, UC-34 Physics, TID-4500 (16th Ed.)

FROM: Technical Information Division

SUBJECT: The Pion-Pion Cross Section by the Chew-Low Method by D. Duane Carmony (Thesis), dated October 1961

Please make the following corrections on your copy of subject report.

Page 2, Fig. 1.	abscissa label: Reads - "P_p(Mev)"	Should Read - "P_p (Mev/c)"
Page 10, Line 8:	Reads - "valve"	Should Read - "value"
Page 10, Eq. (II-4):	Reads - $\pi^+ + \pi^- \rightarrow \pi^+ + \pi^0$	Should Read - $\pi^+ + \pi^0 \rightarrow \pi^+ + \pi^0$
Page 14, Fig. 5:	Reads - "of the scattering amplitude"	Should Read - "of the square of the scattering amplitude"

Page 18, Line 16: Reads - "pi^2 and constant ω^2, ω_i^2 the ....."

Should Read - "p_i^2 and constant ω^2, ω_j^2 the ....."

Page 20, Line 23: Reads - "region and thus"

Should Read - "region and the"

Page 25, Fig. 11: Reads - Legend: "$\pi^- + p \rightarrow p + \pi^+ + \pi^0$ "

Should Read - "$\pi^- + p \rightarrow p + \pi^- + \pi^0$ "

Page 28, Fig. 13: Reads - "ω = 27-33" Should Read - "ω^2 = 27-33"

Reads - "ω = 30" Should Read - "ω^2 = 30"

Page 34, Eq. (C-3) Should Read

$$p_\pi = \sqrt{\frac{(\omega^2+p^2+1)^2}{(2\omega)^2} - 1} = \frac{1}{2\omega} \sqrt{[(p^2+(\omega+1)^2][p^2+(\omega-1)^2]}$$

Page 36, Line 2: Reads - "that the T-spin function"

Should Read - "that the product of the T-spin functions"

Page 36, Line 3: Reads - "(and the T=2 T-spin states . . ."

Should Read - "(and the T=1 T-spin states . . . "

Page 36, Eq. (D-5): Replace A' by A^1.

Page 36, Eq. (D-9):

$$\sigma_{\pi^+\pi^0} = 12\pi \lambda\!\!\!^{-2} = 12\pi/[(\omega^2/4) - 1].$$

Page 36, Line 10: Reads "as $\delta_0{}^2$, $\delta_1{}'$, $\delta_2{}^2$, and $\delta_3{}'$ "

Should read: "as $\delta_0{}^2$, $\delta_1{}^1$, $\delta_2{}^2$, and $\delta_3{}^1$ "

THE PION-PION CROSS SECTION BY THE CHEW-LOW METHOD

D. Duane Carmony

Lawrence Radiation Laboratory
University of California
Berkeley, California

October, 1961

ABSTRACT

By the use of the Alvarez 72-inch hydrogen bubble chamber exposed to a 1.25-Bev/c $\pi^{\pm}$ beam designed by Professor Frank Crawford, a study of the processes $\pi^{+} + p \to p + \pi^{+} + \pi^{0}$ and $\pi^{-} + p \to p + \pi^{-} + \pi^{0}$ has been carried out. All together, 1737 π^{+} and 466 π^{-} events with low momentum transfer to the proton (less than 400 Mev/c) have been measured.

Evidence has been found for a $T = J = 1$ di-pion resonance of mass 730 Mev and full width at half maximum of 150 Mev (total di-pion energy squared = 29 neutral pion masses squared).

The height of the cross section by extrapolation for both the π^{+} and π^{-} data and in the physical region for the π^{+} is consistent with $(2J + 1)\, 4\pi \lambdabar^{2}$ for a p-wave resonance. Angular distributions were determined in the physical region for the π^{+} data. These distributions are strongly dominated by a $\cos^{2}\theta_{\pi\pi}$ term (s-, d-, and f-wave resonances can be ruled out by this experiment).

The π^{-} data do not show the dominance of the single-pion exchange process in the physical region. The cross section $\sigma_{\pi^{-}\pi^{0}}$ as determined by the Chew-Low extrapolation method does show a resonant rise, thus indicating that the applicability of the Chew-Low method is not restricted to situations in which the physical region contains already as much information as one hopes to learn by extrapolation.

I. DATA COLLECTION AND EVENT SELECTION

This experiment, an investigation of the pion-pion interaction by means of the reaction $\pi^{\pm} + p \rightarrow \pi^{\pm} + p + \pi^{0}$, has been carried out at the Lawrence Radiation Laboratory in the Alvarez 72 inch hydrogen bubble chamber with a beam designed by Professor Frank Crawford. The results of an earlier experiment[1,2,3] which led to the experimental verification of a pion-pion resonance indicated that the present beam momentum (1255 Mev/c) would be ideal for studying the properties of this resonance.

A. Data Collection.

1. π^- Film

The scanners searched for non-strange-particle interactions resulting in two-prong events in which one of the tracks was a stopping proton. The only reactions that fulfill these criteria at 1282 Mev/c are

$$\pi^- + p \rightarrow \pi^- + p, \tag{I-1}$$
$$\pi^- + p \rightarrow \pi^- + p + \pi^0, \tag{I-2}$$
$$\pi^- + p \rightarrow \pi^- + p + \geqslant 2\pi^0. \tag{I-3}$$

It is possible to reject most of the elastic events (Eq. 1) on the scanning table without detailed measurements. From Fig. 1 we see that if we restrict ourselves to recoil protons of momentum less than 400 Mev/c, the scattered protons in Reaction (1) have space angles with respect to the beam direction that are greater than 70 deg. On the other hand, the additional neutral in Reaction (2) causes the proton to go forward of 73.5 deg. (lab). Our scanners were trained to make rough measurements (about ± 1% in momentum, ± 2 deg. in space angle) of the momentum and angle of the recoil proton.

The beam enters the chamber as approximately 20 highly parallel tracks. Any beam particle that undergoes Reaction (2) loses at least 135 Mev/c of momentum even if the proton carries off negligible momentum in the laboratory system. This 10% change in curvature relative to the rest of the tracks is readily observed by the scanner, allowing him frequently to detect the interaction point of "zero-length" protons. We have there-

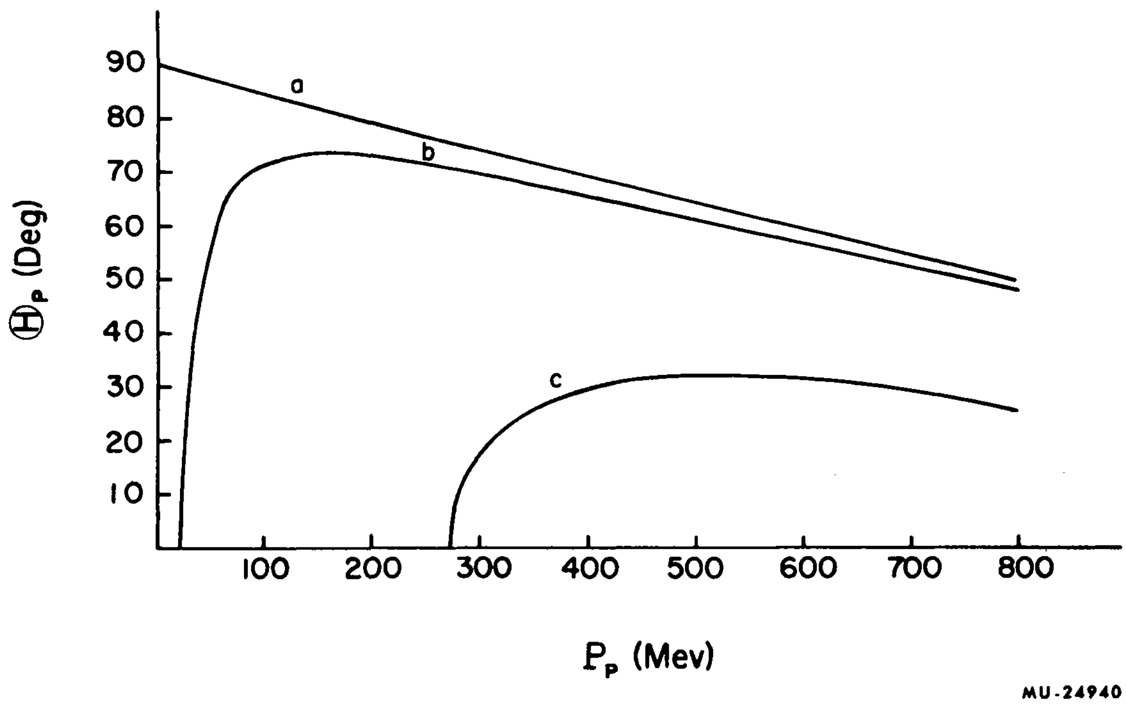

Fig. 1. Kinematics at 1255 Mev/c. Curve a shows the relationship between the lab space angle and the lab momentum of the proton in the elastic reaction $\pi+p\to\pi+p$. Curve b shows the allowed region for the reaction $\pi+p\to p+\pi+\pi^0$. Curve c shows the relationship between Θ_p and P_p for the reaction $\pi+p\to p+\pi^*$, where the mass of π^* is 730 Mev.

fore assumed that the scanning efficiency does not depend upon the length of the proton track seen. We accept no protons of momentum less than 95 Mev/c (range 0.25 cm), in order to assure fulfillment of this important assumption.

2. π^+ Film

The π^+ beam contained a 20-foot electrostatic separator which removed most of the proton contamination. The residual proton contamination. The residual proton contamination was about 2%. (See Appendix A for a discussion of path lengths, scanning efficiencies, and beam contamination.) The possible non-strange-particle interactions with a stopping proton at 1255 Mev/c in the π^+ film are

$$\pi^+ + p \rightarrow \pi^+ + p, \tag{I-4}$$
$$\pi^+ + p \rightarrow \pi^+ + p + \pi^0, \tag{I-5}$$
$$\pi^+ + p \rightarrow \pi^+ + p + \geqslant 2\pi^0, \tag{I-6}$$
$$p + p \rightarrow p + p, \tag{I-7}$$
$$p + p \rightarrow p + p + \pi^0, \tag{I-8}$$
$$p + p \rightarrow p + n + \pi^+. \tag{I-9}$$

Reactions (8) and (9) are negligible because of the low beam contamination and the small inelastic p-p cross sections at this energy. Reactions (7) and (5) are distinguished from (4) by the scanner in the same way as (2) is from (1).

B. Event Selection

In order to determine the total elastic pion-pion cross section, it suffices to measure the laboratory-system momentum and space angle of the scattered proton in Reactions (2) and (5). (See Chapter II, Section B, and Appendix B). Prior to this experiment, scanning-table measurements of these two quantities were carried out on 1700 events at 1.03 Bev/c. Although the table method is not adaptable to the measurement of the differential pion-pion cross section (unless one were to measure the momentum of the secondary pion by using templates) and does not separate out the multiply inelastic events, it was selected initially because it was a rapid way to process events and it was known that the multiple production of neutral pions is less than 10% at 1 Bev/c.[4] This method has now been superseded in this experiment by a Franckenstein-PANG-KICK-EXAMIN-HISTOGRAM system. Even so, we mention the former method briefly because it was the basis of several published reports and because our scanners continued to eliminate elastic-scattering events on the scanning table through the use of this measuring system.

Our "by hand" measurements are based on the method of G. Lynch, which, using the three views of the 72-inch chamber, measures the projected chord length, and the projected angle in the plane of the chamber, and the dip angle of the proton.[5] The proton angle, Θ_p, and the proton momentum, P_p, were tabulated for each event along with certain functions of these variables, $p^2(P_p)$ and $\omega^2(P_p, \Theta_p)$.

In this experiment, however, the data processing was done in the following way. An IBM master card was made for each event found. The events were measured on the Franckenstein and processed through PANG[6] and KICK.[7] A program, EXAM,[8] was written to read KICK tape and place events in categories: failure, nonbeam events, elastic scatterings, inelastic single π^0 production, multiproduction, and "pathological" events. For every valid inelastic single π^0 production, the EXAMIN program program punched a data card which contained all the necessary data for the event (serial number, missing mass, χ^2 for single production, the ratio χ^2_e/χ^2_i (where e and i refer to the hypotheses for elastic and inelastic reactions), henceforth called χ^2 ratio, and certain functions of the fitted angles and momenta). To be processed automatically as a valid inelastic event without an "off-line" physicist, an event has to satisfy the following criteria:

a. The beam momentum is within 50 Mev/c of nominal.

b. There is an uncertainty in the missing mass, ΔM, less than 60 Mev. This value was chosen because it is about three times the error of a typical event and is less than one-half the mass of a pion.

c. $M - \Delta M \lesssim (3/2)\, m_\pi = 210$ Mev, and $M + \Delta M > (1/2)\, m_\pi = 70$ Mev, where M is the missing mass and ΔM is the error in the missing mass (see Fig. 2 for a distribution of the missing mass of those events

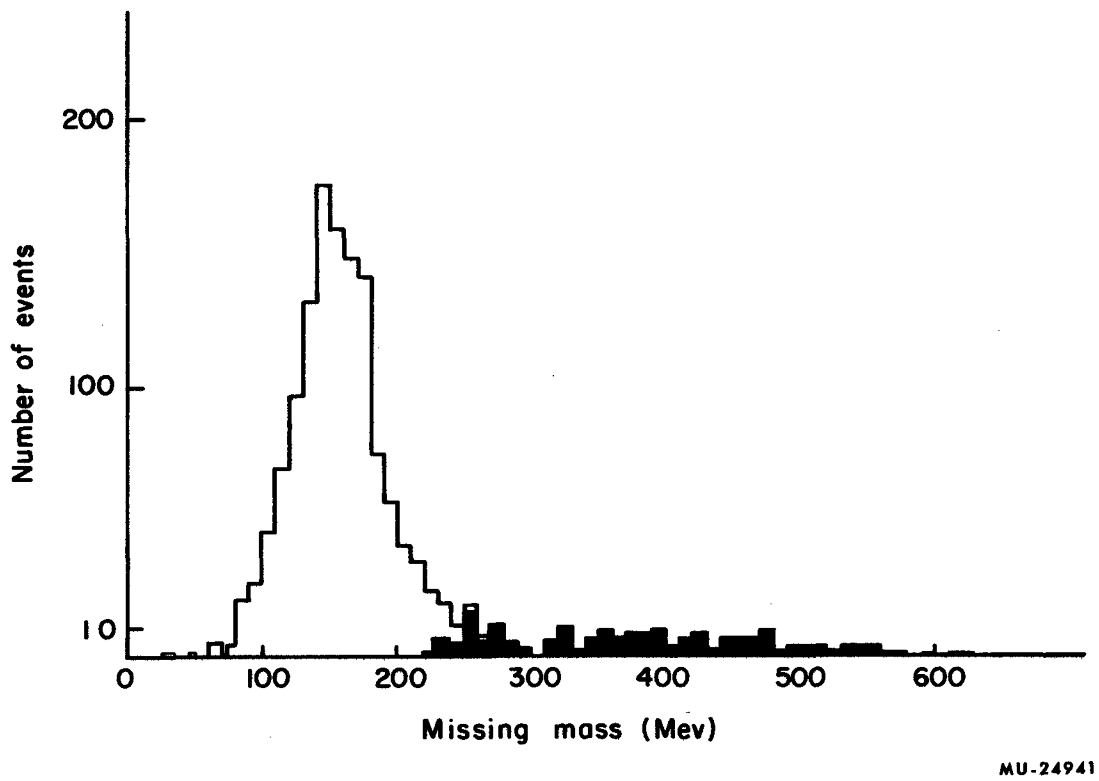

Fig. 2. The missing-mass spectrum of those π^+ events satisfying criteria a, b, c of Chapter I Section B. (The dark shaded events fit multiple π^0 production).

having ΔM less than 60 Mev).

d. The χ^2_i of the "inelastic hypothesis" (one degree of freedom) is less than 20 and the χ^2 ratio greater than 100 (see Fig. 3 for our inelastic event χ^2 distribution).

The sample of events with $M+\Delta M < 70$ Mev was found to be almost entirely elastic events. Any event that did not fit the "elastic hypothesis" with a very high probability (we demanded χ^2_e less than 10, for four degree of freedom) was examined on the scanning table. A few elastic events had $M+\Delta M$ greater than 70 Mev. These were, however, automatically rejected from our sample of inelastic events by the χ^2 ratio test.

About 10 to 15% of our inelastic events are really $2\pi^0$ events. We believe that the requirement $M - \Delta M \leqslant 210$ Mev for a single production allows us a relatively clean sample of single-production events, since the much less abundant multiple production begins with a threshold at 270 Mev.

Events that did not satisfy all the criteria (such as $\Delta M < 60$ Mev, etc.) were ear-marked "pathological" and were examined by a physicist. (More than 90% of the events went automatically through the system; that is, they fulfilled criteria a through d.)

For all events that passed the EXAMIN criteria directly or were aided through by the physicist, the data card replaced the initial master card. For events which were fitted as elastic, non-beam, or multiproduction, a code was punched in the master card. The data cards formed the input for histogram-making programs.

C. Geometrical Corrections

In order to reduce the measuring by almost an order of magnitude we selected inelastic reactions only when the momentum of the proton was less than 400 Mev/c and the proton stopped in the chamber. We then assigned to each event, according to the space angle and momentum of the proton, a statistical weighting factor as computed by an IBM 704 program.[9,10] In order to be accepted each event had to have its interaction point within a fiducial volume and the proton had to stop within the chamber. The program

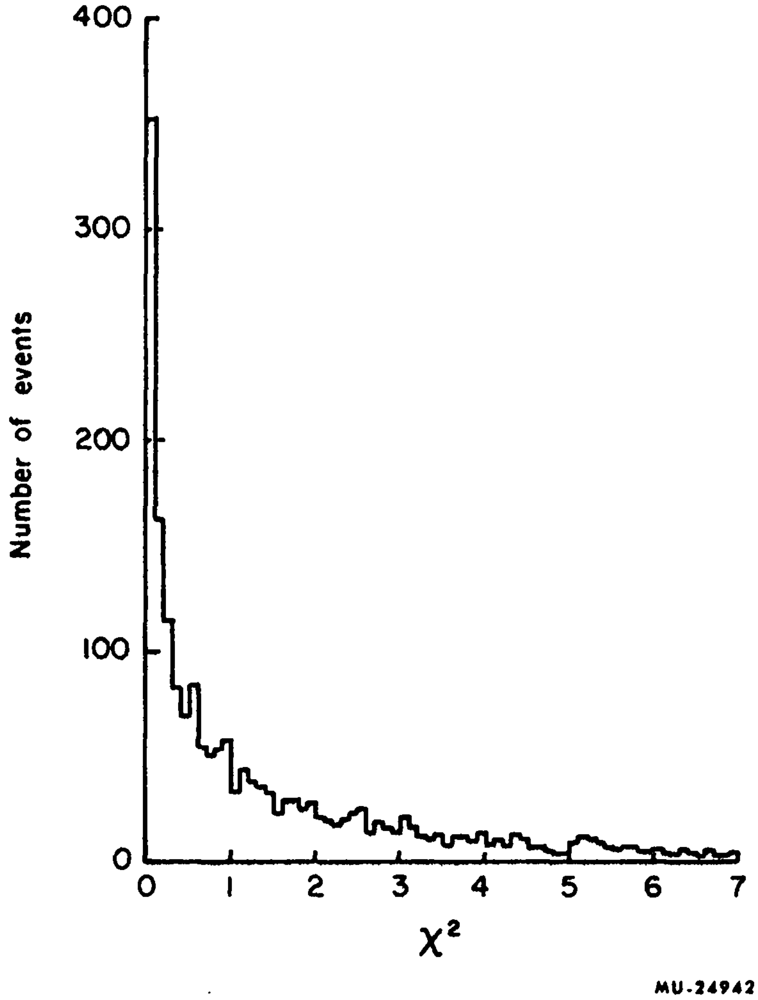

Fig. 3. The χ^2 distribution of all the events ($\pi^{\pm}$) which satisfy criteria a through c of Chapter I Section B (one degree of freedom).

computed, for an ensemble of points spaced evenly over the chamber (but given a weight determined by the experimental beam distribution), that fraction of interactions with a given secondary proton range (momentum) and space angle which stay in the chamber. Table I shows the correction that must be applied to the experimental number of events in order to get the true number of events.

Table I. Escape Correction Factors for the π^+ film.

p^2 / ω^2	1	2	3	4	5	6	7	8
7	1.003	1.018	1.043	1.127	1.361	-	-	-
11	1.001	1.013	1.040	1.109	1.430	-	-	-
15	1.000	1.011	1.038	1.114	1.311	1.616	-	-
21	-	1.007	1.032	1.089	1.171	1.509	-	-
25	-	1.004	1.003	1.069	1.138	1.284	1.781	-
29	-	-		1.055	1.097	1.191	1.385	-
31	-	-		-	1.100	1.154	1.287	1.677
35	-	-		-		1.150	1.232	1.343

Where p^2 and ω^2 (in pion masses) are defined by Eq. II-6 and II-7.

II. THEORETICAL CONSIDERATIONS

A. The Theoretical Prediction of a Pion-Pion Resonance

One reason why it is important to know the pion-pion cross section is because one is able by using dispersion relations, to relate the electromagnetic structure of the nucleon to the pion-pion interaction. This interrelationship occurs because there exists in the dispersion theory for the isotopic vector form factor of the nucleon an integral in t, the square of the momentum transfer over the imaginary part of the form factor. Symbolically,

$$\langle N\bar{N} \mid \gamma \rangle \propto \int_{(2m_\pi)^2}^{\infty} dt' \ \mathrm{Im} \frac{\langle N\bar{N} | \gamma \rangle}{(t' - t)} , \qquad \text{(II-1)}$$

where the limits of integration run from a lower limit to infinity, and where the lower limit is determined by the lowest-mass system consisting of strongly interacting particles that has the same quantum numbers as a gamma ray--that is, zero baryon number, zero strangeness, and angular momentum $J = 1$. The lowest-mass system fulfilling these criteria is two pions in a p state.

In the dispersion formulation the form factor is most strongly affected by the behavior of the lowest-mass system. Frazer and Fulco showed that if one postulates a strong p-state di-pion resonance the experimentally found nucleon electromagnetic structure can be understood.[11]

This interrelationship can be qualitatively understood as follows: Expand the imaginary part of the nucleon form factor as a sum over intermediate states and keep only the lightest intermediate state, the two-pion state:

$$\mathrm{Im} \langle N\bar{N} \mid \gamma \rangle = \langle N\bar{N} \mid \pi\pi \rangle \langle \pi\pi \mid \gamma \rangle + \cdots . \qquad \text{(II-2)}$$

Here $\langle N\bar{N} \mid \pi\pi \rangle$ is related to the pion-nucleon scattering amplitude $\langle \pi N | \pi N \rangle$ through crossing symmetry; $\langle \pi\pi | \gamma \rangle$ is the pion electromagnetic form factor. Thus Eq. (1) relates the nucleon form factor to the pion-nucleon phase shifts and to the pion form factor.

The pion form factor itself satisfies a dispersion relation, and, again expanding only to the lowest-mass system having the same quantum numbers as two pions in a p state (namely, two pions in a p state), one obtains an integral equation for the pion form factor involving $\langle \pi\pi | \pi\pi \rangle$ and $\langle \pi\pi | \gamma \rangle$. Specification of the pion-pion phase shifts, $\langle \pi\pi | \pi\pi \rangle$, results in a valve for the nucleon form factor. Frazer and Fulco showed that the experimental nucleon form factor can be explained if they assume a di-pion resonance in the $T = J = 1$ state, and they give the following two-parameter formula for the phase shift δ_1^1:

$$|e^{i\delta_1} \sin \delta_1^1|^2 = \frac{\Gamma^2}{\left(\frac{\nu+1}{\nu^3}\right)\left(\nu_r - \nu[1-\Gamma a(\nu)]\right)^2 + \Gamma^2}, \qquad \text{(II-3)}$$

where Γ and ν_r are parameters and where ν = square of the momentum of each pion (in the di-pion rest system, in units $\hbar = c = m_\pi = 1$) and

$$a(\nu) = (2/\pi)[\nu/(\nu+1)]^{1/2} \ln[\nu^{1/2} + (\nu+1)^{1/2}] .$$

The original prediction by Frazer and Fulco was that there should be a pion-pion $T = J = 1$ resonance at a di-pion total mass squared of about $11\, m_\pi^2$ (that is, $\nu_r = 1.5$, $\Gamma = .4$).

Bowcock, Cottingham, and Lurie, using a subtracted dispersion relation for the nuclear form factor and more recent data on electron-nucleon scattering, predicted that the resonance should occur at total di-pion mass squared of $22.4\ m_\pi^2$.[12]

B. The Chew-Low Extrapolation Method

The Chew-Low method[13] is well suited to the study of the pion-pion interaction because it allows us to determine the cross section for the process

$$\pi^+ + \pi^- \rightarrow \pi^+ + \pi^0 \qquad \text{(II-4)}$$

from the study of the reaction

$$\pi^{+} + p \to p + \pi^{+} + \pi^{0} \qquad \text{(II-5)}$$

In order to determine the pion-pion cross section from Reaction (5) it is necessary to study events in which spectator proton receives little momentum transfer in the pion-proton collision. The physical content in this requirement is that the small momentum transfer to the proton implies a large impact parameter, that is, the π^{+} has collided with a virtual neutral pion in the tail of the mesonic cloud which surrounds the proton. This type of peripheral collision is illustrated in Fig. 4(a).

In order to measure the total elastic pion-pion cross section it suffices to determine two quantities for each event of Reaction (5). These two quantities are the invariant four-momentum transfer, p, of the spectator proton, and the invariant mass of the di-pion system, ω. These invariants are given in terms of laboratory-system quantities by

$$p^{2} = (0-P_{p})^{2} - (m - \sqrt{m^{2} + P_{p}^{2}})^{2} \qquad \text{(II-6)}$$

and

$$\sqrt{P_{in} + m_{\pi}^{2}} + M = \sqrt{P_{p}^{2} + m^{2}} + \sqrt{(\underline{P}_{in} - \underline{P}_{p})^{2} + \omega^{2}}, \qquad \text{(II-7)}$$

where M = mass of the proton, m_{π} = mass of the pion P_{in} = momentum of the incident pion, and P_{p} is the laboratory-system momentum of the proton. Defining $\cos \Theta_{p} = \hat{\underline{P}}_{in} \cdot \hat{\underline{P}}_{p}$, we see that we have

$$P^{2} = P^{2}(P_{p}), \qquad \text{(II-8)}$$

and

$$\omega^{2} = \omega^{2}(P_{p}, \Theta_{p}). \qquad \text{(II-9)}$$

If Fig. 4a were the only diagram for the process $\pi + p \to p + \pi + \pi^{0}$, then the amplitude for Eq. (4) and (5) would be related by

$$|A_{\pi p - p\pi\pi}|^{2} = \left| \frac{\Gamma_{\pi n} A_{\pi\pi \to \pi\pi}}{p^{2} + m_{\pi}^{2}} \right|^{2} \propto \frac{f^{2} p^{2} |A_{\pi\pi}|^{2}}{(p^{2} + m_{\pi}^{2})^{2}}, \qquad \text{(II-10)}$$

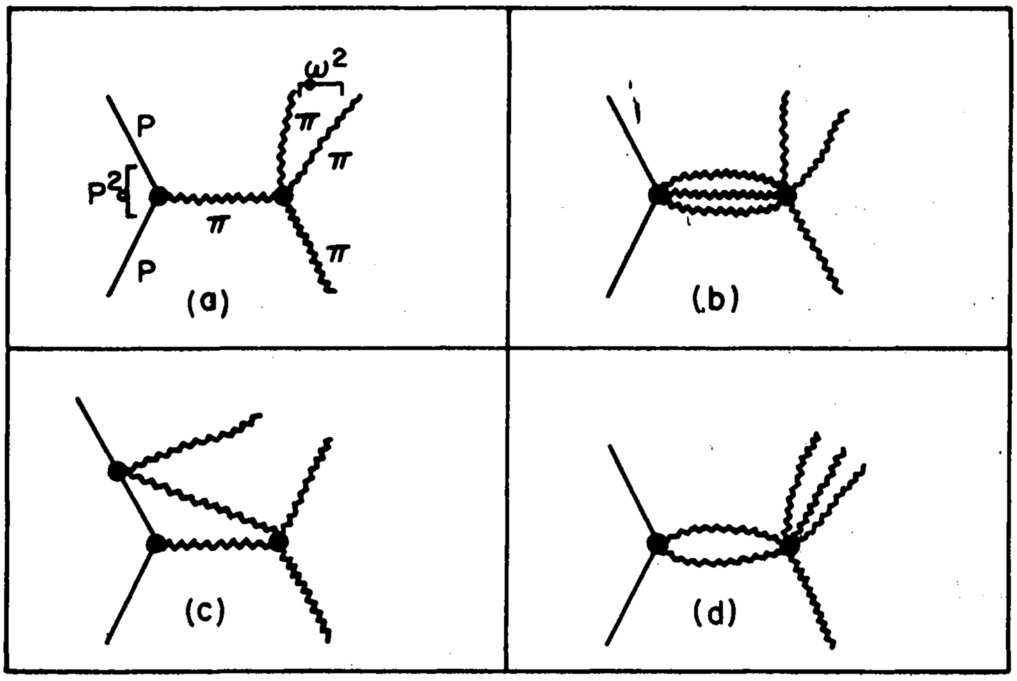

MU-24943

Fig. 4. Here (a) is the single-pion production diagram which produces a pole in the pion-nucleon scattering amplitude; (b) and (c) are examples of contributions to the branch cut; (c) is also an example of a final-state interaction; (d) represents the nearest singularity in the case of double π^0 production.

where $\Gamma_{\pi n}$ is the pion-nucleon vertex function, $1/(p^2 + m_\pi^2)$ is the pion propagator, and the A's are the amplitudes of Reactions (4) and (5): $\Gamma_{\pi n}^2 = f^2 p^2 / m_\pi^2$, where $f^2 = .08$. We adopt the units $\hbar = c = 1$ and the mass of the neutral pion = 1.

The amplitude $A_{\pi p}$ considered as an analytic function of the square of the invariant four-momentum transfer, p^2, has a pole at $p^2 = -1$ because of the process shown in Fig. 4(a). The analytic structure of $A_{\pi p}$ for fixed ω^2 is given in Fig. 5(a). The branch cut running from $p^2 = -9$ to $-\infty$ comes about from all the other pion-exchange diagrams leading to the final state $p + \pi + \pi^0$, for example, Fig. 4(b) and (c).

Chew and Low[13] give the following prescription for determing the pion-pion cross section, $\sigma_{\pi\pi}$ (see appendix B for a discussion of this formula).

Determine the two-dimensional distribution $d^2\sigma_{\pi p}(p^2, \omega^2)/dp^2 d\omega^2$, where $\sigma_{\pi p}$ is the cross section for the process $\pi + p \rightarrow \pi + p + \pi^0$. The value of the function $(p^2+1)^2 \cdot d^2 \sigma_{\pi p}(\omega^2, p^2)/ dp^2 d\omega^2$ extrapolated to $p^2 = -1$ is proportional to $\sigma_{\pi\pi}(\omega^2)$. The formula given by Chew and Low is

$$\lim_{p^2=-1} (p^2+1)^2 d^2\sigma_{\pi p}/dp^2\, d\omega^2 = \frac{p^2 f^2}{2\pi P_{in}^2} \cdot \omega[\omega^2/4 - 1]^{1/2} \cdot \sigma_{\pi\pi}(\omega^2) , \tag{II-11}$$

where p^2, ω^2, and P_{in} (which is the lab momentum of the incident pion) are all expressed in units of the neutral pion mass.

The function $(p^2+1)^2\, d^2\, \sigma_{\pi p}/dp^2 d\omega^2$ is analytic in the p^2 complex plane in a circle of radius $p^2 = 8$ about the point $p^2 - 1$. We therefore expand the function as follows:

$$(p^2+1)^2 d^2\sigma_{\pi p}/ d\, p^2 d\omega^2 = A_0 + A_1(p^2+1) + A_2(p^2+1)^2 + \cdots . \tag{II-12}$$

We have used such an expansion in the physically accessible region $p^2 = p^2_{min}$ to $p^2 = 7$ (where p^2_{min} is determined by the incident beam momentum; see Fig. 6). Evaluation of the coefficient A_0 gives us the

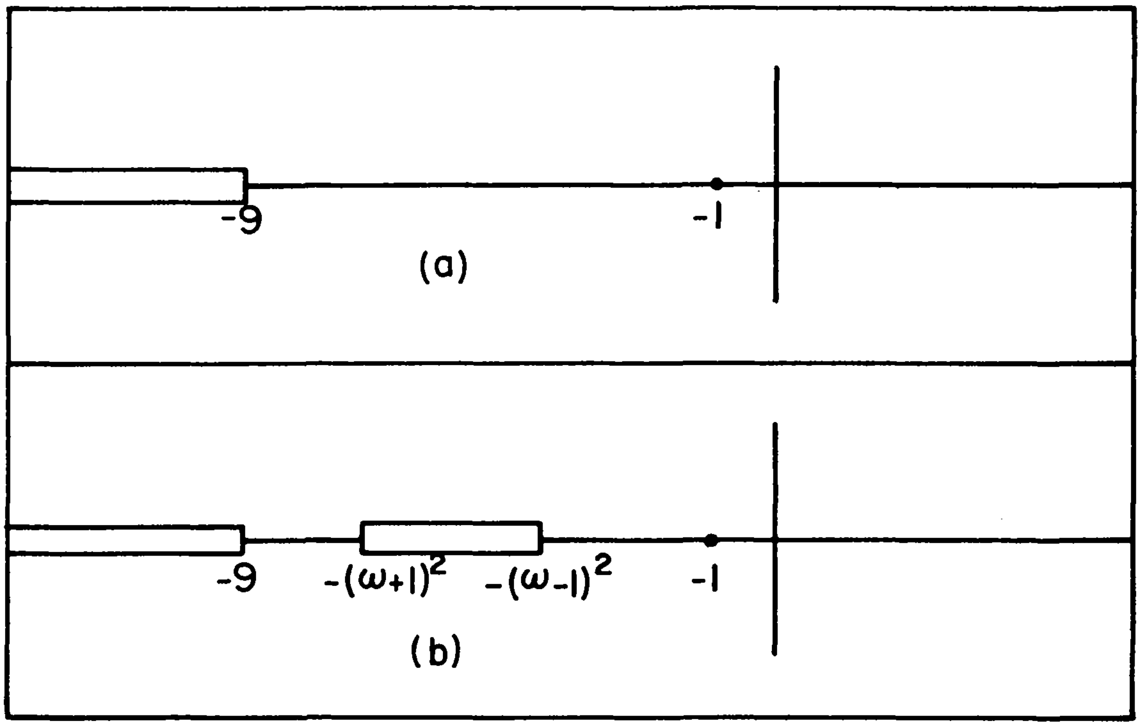

MU-24944

Fig. 5. Here (a) shows the conjectured analytic structure of the scattering amplitude $A_{\pi p \to p \pi\pi}$ for the extrapolation to the total pion-pion cross section; (b) shows the conjectured structure for extrapolation to the differential pion-pion cross section.

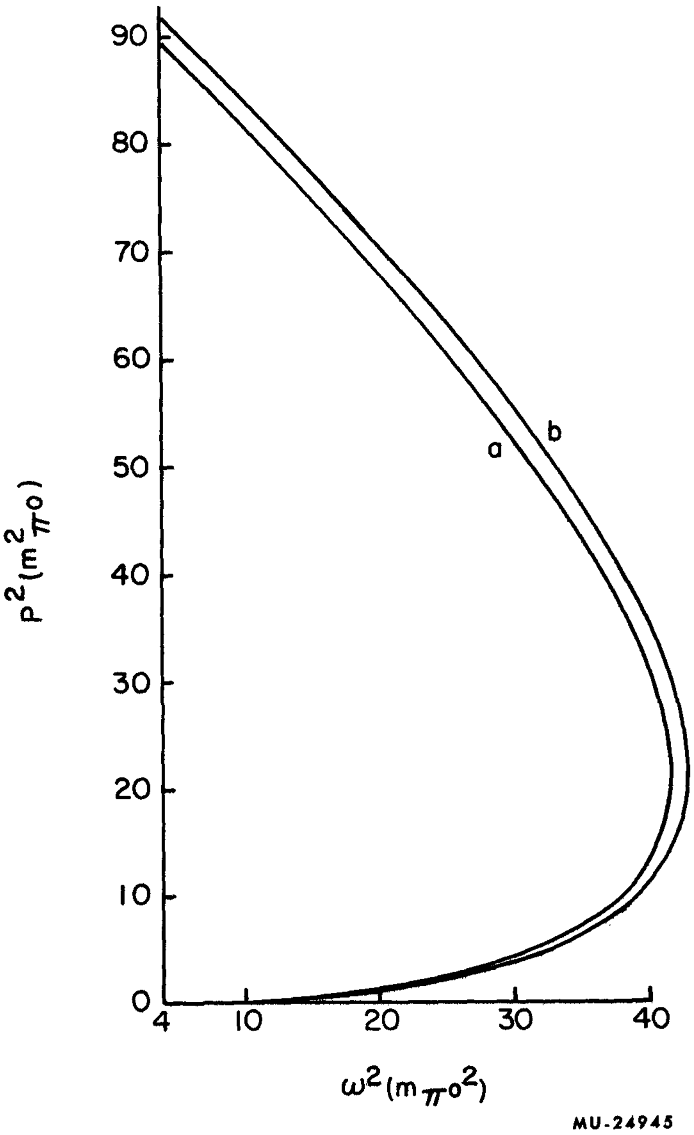

Fig. 6. The kinematically allowed region p^2 vs ω^2 for incident pion beam momenta of 1255 Mev/c and 1282 Mev/c.

pion-pion cross section:

$$\sigma_{\pi\pi}(\omega^2) = - A_0(\omega^2) \cdot \frac{2\pi P_{in}^2}{f^2} \cdot \omega[\omega^2/4] - 1)^{1/2} . \qquad \text{(II-13)}$$

Theory does not tell us at what order we should cut off Eq. (12). We have fitted polynomials in $(p^2 + 1)$ to the fourth order, and have chosen for each extrapolation (i.e., each band of constant ω^2 the lowest-order fit that gave χ^2/M (where M is the number of degrees of freedom) of the order of unity. The χ^2 probability of each of our fits is shown in Table II. Linear fits were satisfactory in this experiment for all ω^2 bands.

We wish to emphasize the following two points. Since the pion-proton cross section is positive definite, the extrapolation(curves as will be seen in Fig. 7) must remain positive for p^2 greater than p^2_{min}. This criterion is automatically satisfied by all our fits, except $\omega^2 = 6$ to 10, which violates this constraint by a negligible amount. In previous work by J. A. Anderson, V. X. Bang, P. G. Burke, D. D. Carmony, and N. Schmitz, the linear fits for small ω^2, which were rejected on the basis of χ^2/M, went negative too soon and the quadratic fit for the smallest ω^2 interval (5 to 8.2) violated this constraint by a very small amount. We did not have sufficient data to know whether this quadratic fit would have been replaced by a cubic satisfying this requirement.[3]

Secondly, if the single-pion exchange mechanism were to dominate the reaction $\pi + p + p + \pi + \pi^0$, extrapolation would not be necessary. Such a bold assumption can be tested <u>experimentally</u>. Assume the complete dominance of the diagram shown in Fig. 4a. Then Eq. (11) is exact without the limiting process; that is,

$$(p^2+1)\, d^2 \sigma_{\pi p}/dp^2\, d\omega^2 = \frac{p^2 f^2 \omega[\omega^2/4] - 1)^{1/2}}{2\pi P_{in}^2} \sigma_{\pi^+\pi^0}(\omega^2), \qquad \text{(II-14)}$$

but equating coefficients of p^2 with

$$(p^2+1)^2\, d^2\sigma_{\pi p}/dp^2\, d\omega^2 = A_0 + A_1(p^2+1)\, A_2(p^2+1)^2 + \cdots , \qquad \text{(II-15)}$$

Table II. Results of extrapolation

$\Delta\omega^2$ $(m_\pi^2 0)$	Type of fit	σ (mb)	$\Delta\sigma$ (mb)	χ^2	Degrees of free-dom, M	χ^2 prob-ability (%)
$(\pi^+ \pi^0)$						
6-10	lin.	43.	15.	5.2	5	42
	quad.	69.	46.	4.8	4	30
10-14	lin.	53.	13.	7.0	5	22
	quad.	120.	44.	4.4	4	36
14-18	lin.	62.	16.	3.6	5	60
	quad.	52.	49.	3.6	4	46
18-22	lin.	80.	24.	12.7	8	13
	quad.	224.	85.	9.6	7	21
22-26	lin.	93.	62.	3.1	6	80
	quad.	609.	347.	0.8	5	97
26-30	lin.	260.	117.	3.3	6	77
	quad.	1200.	650.	1.3	5	94
$(\pi^- \pi^0)$						
6-18	lin.	17.	4.	3.2	5	67
	quad.	19.	12.	3.2	4	54
18-22	lin.	24.	12.	1.6	3	66
	quad.	82.	51.	0.2	2	90
22-26	lin.	73.	30.	3.9	6	70
	quad.	57.	170.	3.9	5	58
26-30	lin.	68.	55.	1.4	6	97
	quad.	105.	300.	1.4	5	93
$(\pi^\pm \pi^0)$						
6-10	lin.	27.	8.	4.6	4	34
	quad.	19.	28.	4.5	3	21
10-14	lin.	38.	7.	6.2	5	29
	quad.	58.	23.	5.3	4	26
14-18	lin.	39.	8.	3.2	5	67
	quad.	42.	26.	3.2	4	52
18-22	lin.	51.	13.	13.9	9	13
	quad.	129.	46.	10.8	8	22
22-26	lin.	92.	33.	2.6	6	86
	quad.	313.	188.	1.2	5	95
26-30	lin.	161.	57.	3.0	6	80
	quad.	616.	336.	1.3	5	93
30-34	lin.	-153.	181.	0.9	4	92
	quad.	-2000.	2000.	1.0	3	80

we see that then $A_0 = -A_1$ and $A_2 \ldots = 0$. That is, the fit is linear in (p^2+1) and the extrapolation curve passes through the point $p^2 = 0$. Although Anderson, Burke, Carmony, and Schmitz needed only linear fits in the resonant region, their extrapolation did not go through the origin and the single-pion exchange mechanism did not dominate their physical-region plots.[3]

In this experiment the π^+ data fulfilled the requirements of linear fits and the extrapolaltion curves pass very nearly through the point $p^2 = 0$. We therefore expect to be able to study the pion-pion interaction without extrapolation in the 1255-Mev/c π^+ film.

C. The Pion-Pion Cross Section in the Physical Region

Under the assumption of the dominance of the single-pion exchange diagram, we have, from Eq. (14),

$$\sigma_{\pi\pi} = \frac{2\pi P_{in}^2}{f^2 \omega(\omega^2/4-1)^{1/2}} \frac{(p^2+1)^2}{p^2} \frac{d^2\sigma_{\pi p}}{dp^2 d\omega^2} . \qquad \text{(II-16)}$$

Dividing our data into a two-dimensional histogram in p^2 and ω^2, we have for constant p^2, p_i^2 and constant ω^2, ω_i^2 the following relationship between cross section (in millibarns) and the experimental number of counts N'_{ij} (p_i^2, ω_j^2), in that histogram interval (where the prime indicates that the experimental number of events has been corrected for the finite size of the bubble chamber):

$$\sigma_{\pi p}^{ij} = \frac{N'_{ij}(p_i^2, \omega_j^2)}{L\rho A\delta p^2 \delta\omega^2} \times 10^{-27}, \qquad \text{(II-17)}$$

where L = path length scanned (cm), ρ = density of liquid hydrogen, ρ = .0586 g /cm^3 and A = Avodagro's number.
Therefore we have

$$\sigma_{\pi\pi}^{i}(\omega_j^2) = \frac{2\pi \cdot 10^{-27} P_{in}^2}{f^2 L\rho A\delta p^2 \delta\omega^2} \frac{1}{[\omega_j^2(\omega_j^2/4-1)]^{1/2}} \frac{(p_i^2+1)^2}{p_i^2} N'_{ij}(p_i^2, \omega_j^2), \qquad \text{(II-18)}$$

or, averaging over a series of p^2 bands (all of width δp^2), we find an expression for the di-pion cross section in the physical region, $\sigma_{\pi\pi}^{P}$:

$$\sigma_{\pi\pi}^{P}(\omega_j^2) = \frac{2\pi 10^{-27} P_{in}^2}{f^2 L\rho A\delta p^2 \delta\omega^2 \omega_j(\omega_j^2/4-1)^{1/2}} \frac{1}{n} \sum_{i=1}^{n} \frac{(p_i^2+1)^2}{p_i^2} N'_{ij} . \tag{II-19}$$

D. The Differential Pion-Pion Cross Section

In order to determine the differential pion-pion cross section, $d\sigma_{\pi\pi}/d\cos\theta_{\pi\pi}$. Where $\theta_{\pi\pi}$ is the scattering angle of the charged pion in the c.m. of the reaction $\pi^+ + \pi^0 \rightarrow \pi^+ + \pi^0$, we introduce the following notation. Let q_π be the four-momentum of the charged pion before the collision and q'_π be the four-momentum after the collision. Then we can evaluate the scalar quantity $q_\pi q'_\pi$ in the di-pion c.m. and in the laboratory frame of reference:

$$q_\pi q'_\pi = p_\pi p'_\pi \cos\theta_{\pi\pi} - \epsilon_\pi \epsilon'_\pi = P_{in} P'_\pi \cos\Theta_{\pi\pi} - E_\pi E'_\pi \tag{II-20}$$

where

$$\epsilon'_\pi = \omega/2, \qquad p'_\pi = (\epsilon'^2_\pi - 1)^{1/2}, \tag{II-21}$$

and

$$\epsilon_\pi = \frac{\omega^2 + p^2 + 1}{2\omega}, \qquad p_\pi = (\epsilon_\pi^2 - 1)^{1/2} . \tag{II-22}$$

Thus $\theta_{\pi\pi}$ is given in terms of p^2, ω^2 (which are functions of the lab momentum and angle of the proton) and laboratory-system quantities associated with the charged pion.

As was pointed out by Nauenberg, there is an additional branch cut introduced into the scattering amplitude of the process $\pi+p\rightarrow p+\pi+\pi^0$ (see Appendix C).[14]

III. EXPERIMENTAL RESULTS

We have found evidence for the existence of a π-π resonance of di-pion mass square equal to 29 $m_{\pi^0}^2$ (27 $m_{\pi^+}^2$ or a mass of 730 Mev), and have determined differential cross sections that are strongly indicative of the quantum numbers $T = J = 1$.[15] Thus the isotopic vector form factor of the nucleon can no longer be considered anomalous.

Furthermore, we have evidence for this resonance not only by extrapolation but also by using physical-region plots (essentially Q-value plots). This work is therefore an experimental verification of the importance of the single-pion exchange mechanism, and serves as a further verification of the Chew-Low Method.[16] This work and the work of Anderson, Burke, Bang, Carmony, and Schmitz[3] shows that the usefulness of the Chew-Low extrapolation method is not restricted to situations in which the physical region contains already as much information as one hopes to learn by extrapolation.

A. Results of Extrapolation

The results of the extrapolation are given in Figs. 7, 8, and 9, and in Table II. We see that the π-π cross section, which is very small at low energies,[17] rises to about $12\pi\lambda\!\!\!^{-2}$ (indicative of a p-wave resonance) in the region ω^2 = 26 to 30. The results of the π^+ extrapolation are very consistent with those found in the π^+ physical region plot (Fig. 10). The π^- physical region plot (Fig. 11) is extremely distorted and washed out. Nevertheless, in the region of the resonance, the π^- extrapolation gave results in agreement with the π^+ physical region and thus π^+ extrapolation (see Fig. 8 and Table II).

B. Results in the Physical Region

Since the π^+ extrapolation curves are linear and pass very nearly through $p^2 = 0$, we are allowed to assume that π^+ physical-region plots are reasonable approximations to the true pion-pion cross section. The π^+ physical region peaks at $\omega^2 = 29\ m_{\pi^0}^2$ (with 70% of $12\pi\lambda\!\!\!^{-2}$), and the

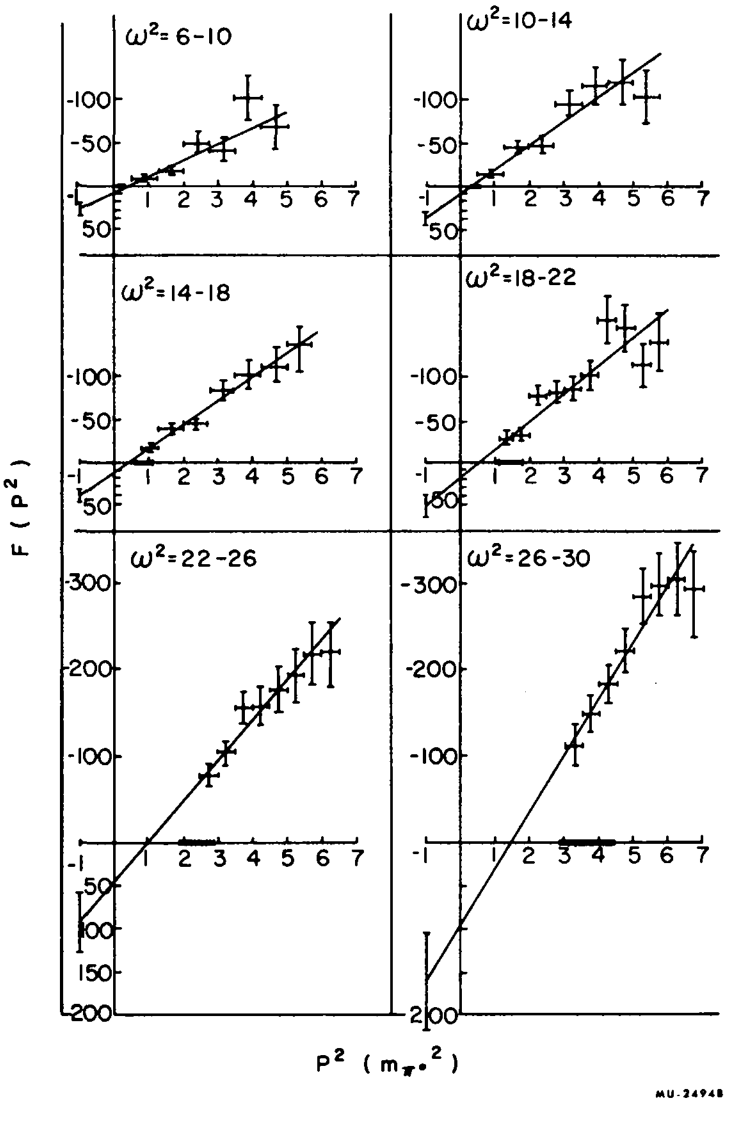

Fig. 7. Extrapolation curves for the combined data, $\pi^+ + p \to p + \pi^+ + \pi^0$ and $\pi^- + p \to p + \pi^- + \pi^0$. Here $F(p^2)$ is normalized to $\sigma_{\pi\pi}$ at $p^2 = -1$.

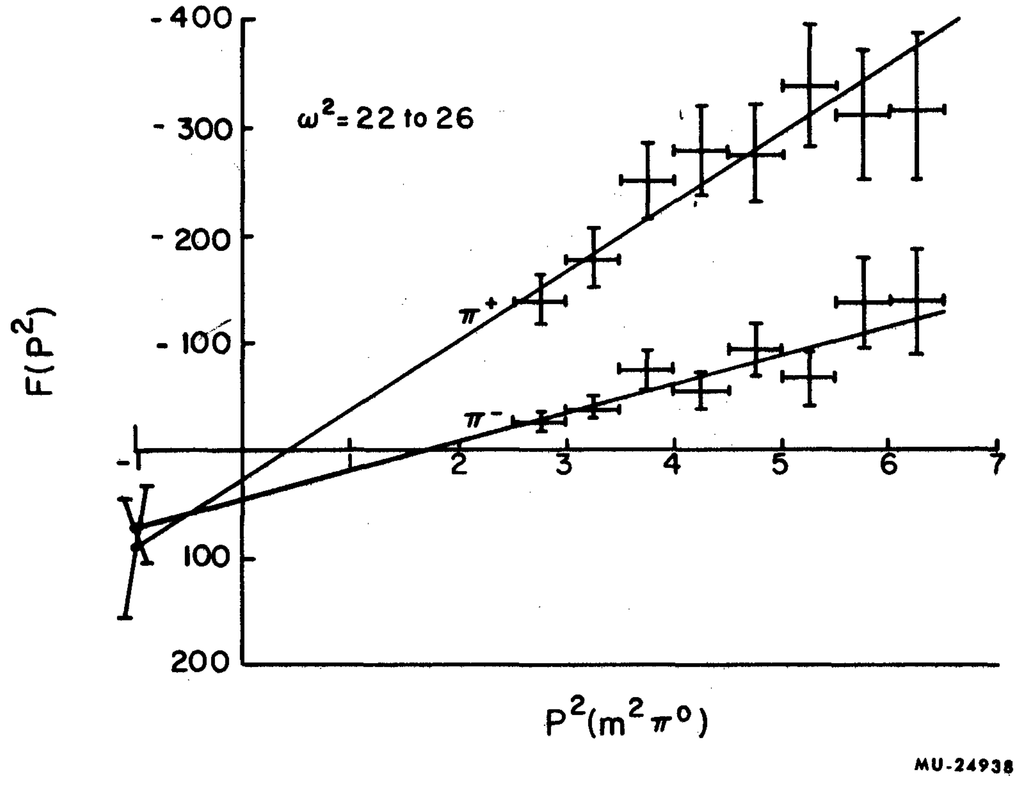

Fig. 8. A comparison of the π^+ and π^- extrapolation curves.

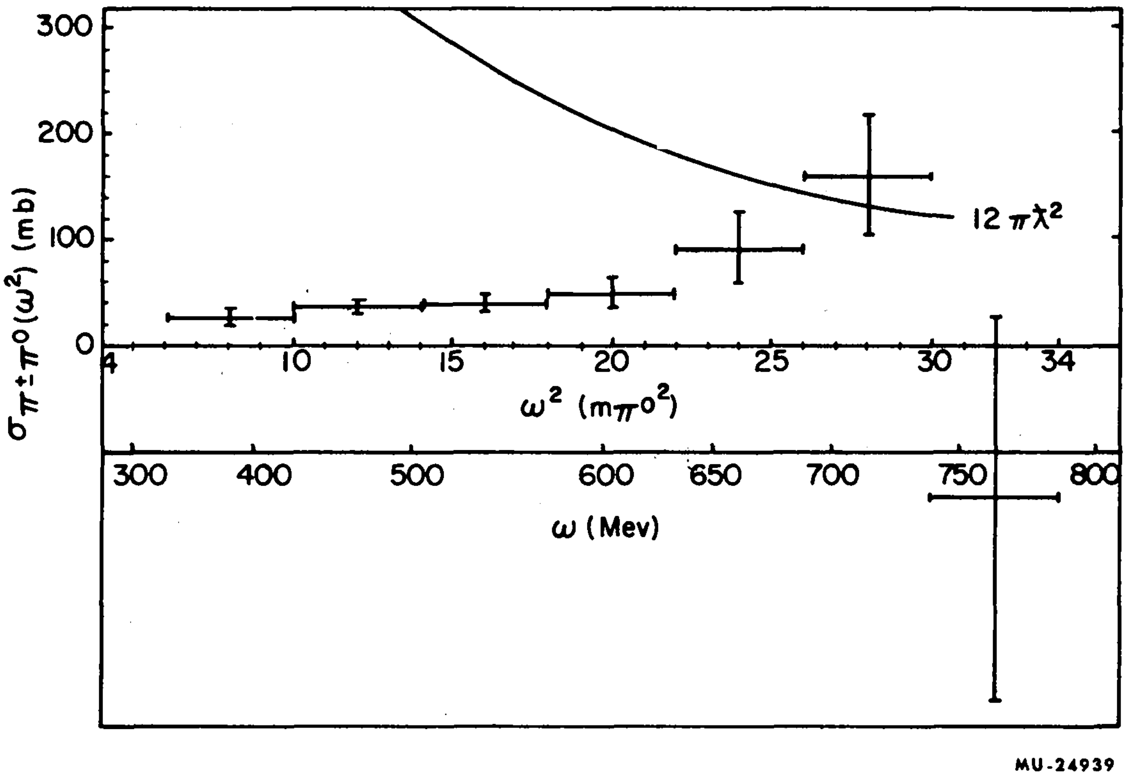

Fig. 9. The total elastic pion-pion cross section (50% I = 1 and 50% I = 2) as a function of the di-pion total energy squared (also as a function of the total mass, in Mev.)

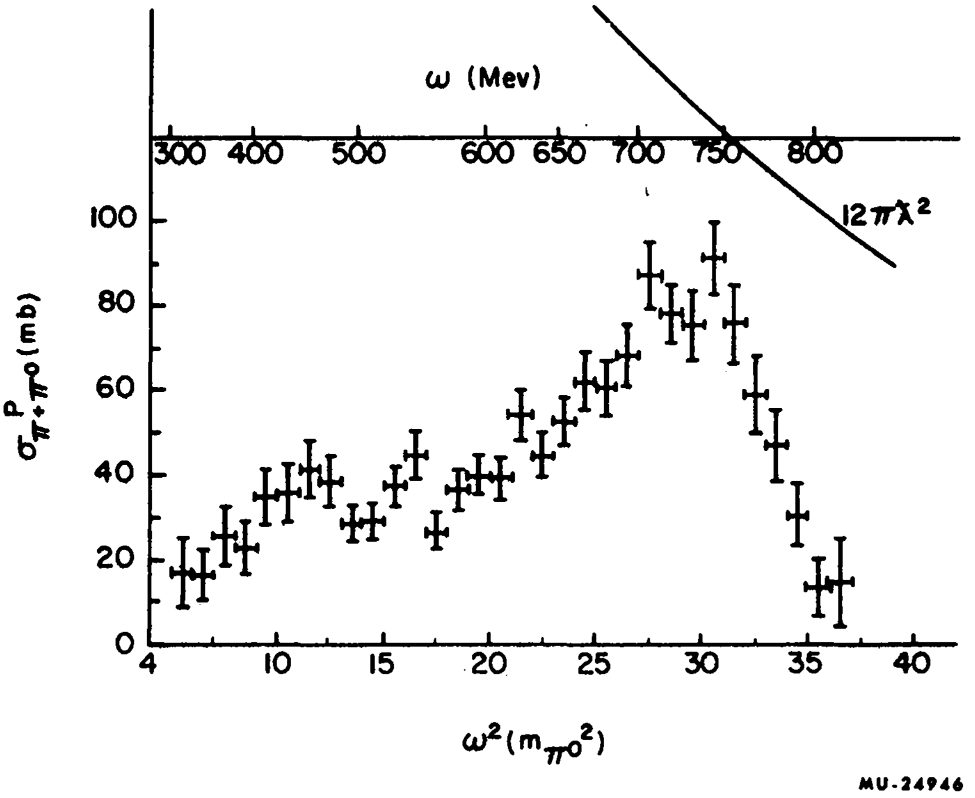

Fig. 10. The total pion-pion cross section as a function of the di-pion total energy squared (in $m^2_{\pi^0}$) as determined in the physical region from the reaction $\pi^+ + p \to p + \pi^+ + \pi^0$ (also as a function of the total mass in Mev.)

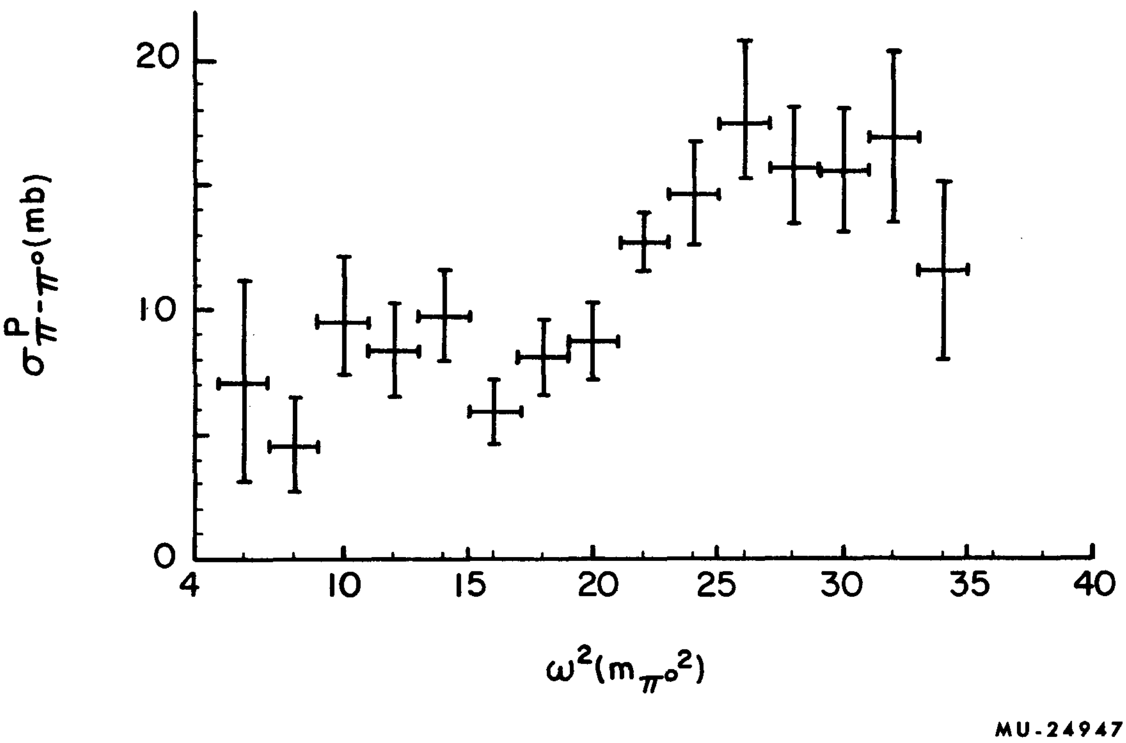

Fig. 11. The total pion-pion cross section as a function of the di-pion total energy squared, as determined in the physical region from the reaction $\pi^- + p \rightarrow p + \pi^+ + \pi^0$.

resonance has a half width at half maximum of 7 $m_{\pi^0}^2$ on the low-energy side and 5 $m_{\pi^0}^2$ on the high side. (The low side especially may be somewhat narrower if a nonresonant background is subtracted.) This corresponds to a resonance at 730 Mev with a full width at half maximum of 155 Mev. It must be remembered that a width so determined is only an approximation. The position and width are in complete agreement with the extrapolation and with the results of other workers.[18]

The results of the differential cross section in the physical region are presented in Figs 12 and 13. Comparison of the experimental data in Fig. 13 with the theoretical predictions for an s-, p-, or d-wave resonance clearly rules out s or d waves. The height of the cross section by extrapolation rules out higher-order waves. Thus the resonance has the quantum numbers T = J = 1. A least-squares fit in ascending orders of $\cos\theta_{\pi\pi}$ was carried out on the data of Fig. 13. The first fit to give a χ^2 probability of 1% or greater was

$$d\sigma_{\pi\pi}/d\cos\theta_{\pi\pi} = (6.9 \pm 0.7) - (1.0 \pm 1.4)\cos\theta_{\pi\pi} + (26.4 \pm 2.4)\cos^2\theta_{\pi\pi}, \tag{III-1}$$

which clearly indicates the dominance of the $\cos^2\theta_{\pi\pi}$ term (the angular distribution for pion-pion scattering in a p state is $\cos^2$, not $3\cos^2 - 1$, as in the case of pion-nucleon scattering; see Appendix D).

Furthermore, if the nonresonant part of the cross section can be described as s-wave scattering, then Fig. 12 indicates that the sign of δ_1^1 and δ_0^2 is the same (see also Eq. AIV-7)

C. Unresolved Experimental Results

The distortion of the physical-region plot in the π^- data is not understood. It is known that Walker et al see about 75% of $12\pi\lambda\!\!\!^{-2}$ at 1.9 Bev/c, using the π^- reaction. It has been pointed out by Professor Frank Crawford that the reaction $\pi^- + p \rightarrow p + \pi^- + \pi^0$ can also go through the intermediate channel $\pi^-\pi^+n$. The reaction $\pi^+ + p \rightarrow p + \pi^+ + \pi^0$ can not go through any intermediate channel consisting of a nucleon and two pions

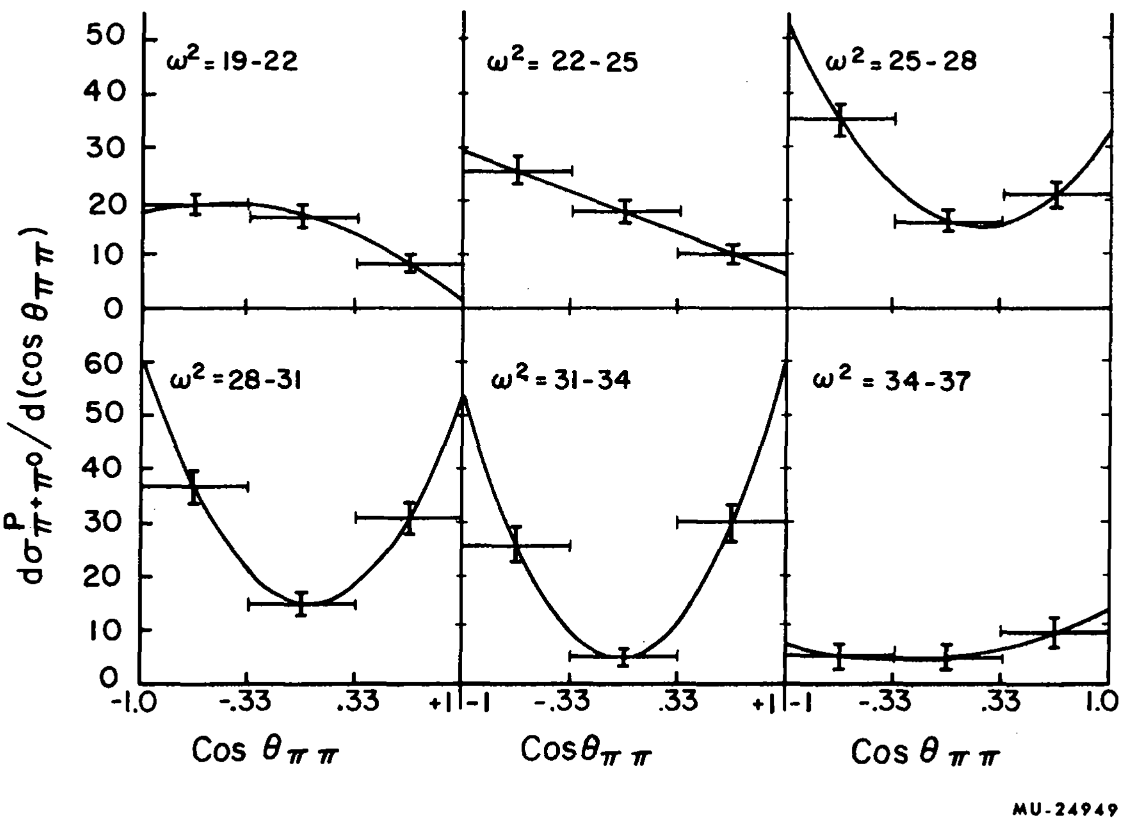

Fig. 12. The differential pion-pion cross section as a function of the di-pion total energy squared, as determined in the physical region.

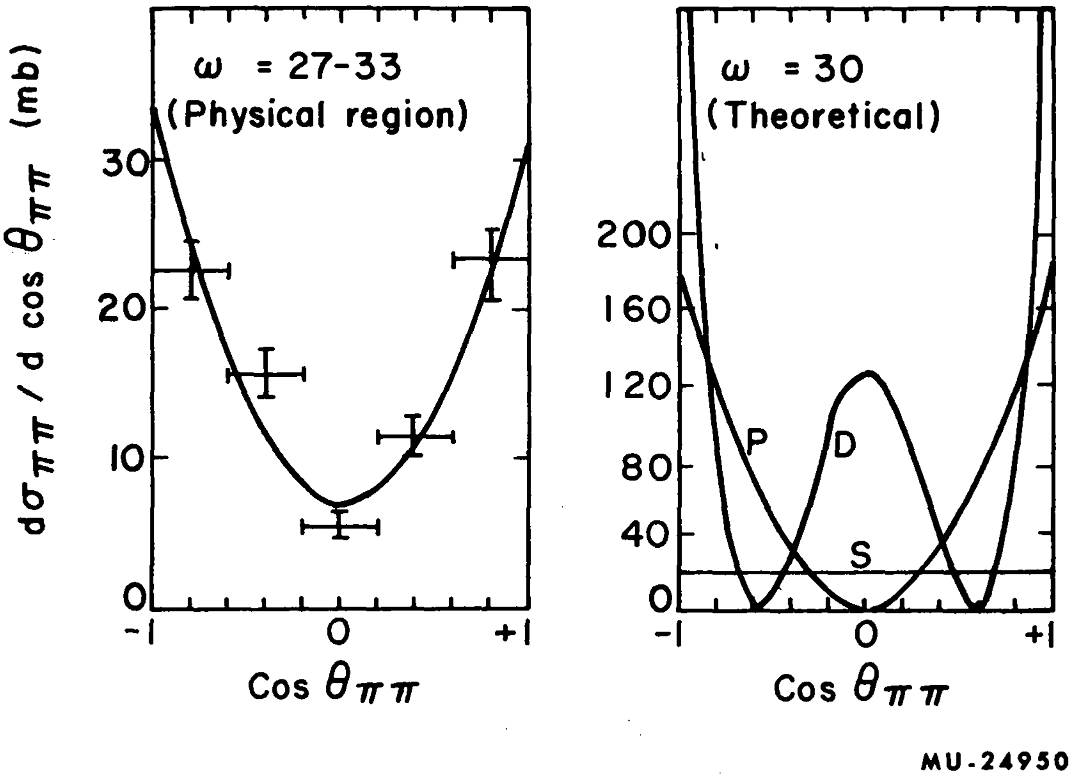

Fig. 13. Here (a) the differential pion-pion cross section as a function of the di-pion total energy squared as determined in the physical region. (b) Theoretical curves for s, p, and d waves.

in a p state. Thus the very dominance of the combination of two pions in a p state could be responsible for the distortion of the physical region observed in this experiment and by Anderson, Burke, Bang, Carmony, and Schmitz at 1030 Mev/c.[3]

ACKNOWLEDGMENTS

I want to thank Professor Luis W. Alvarez for his encouragement and interest in this project and for all the opportunities and stimulation that he and his group have provided. I am grateful to Professor Frank S. Crawford, Jr., who designed the beam used in this experiment, for much valuable criticism and discussion. I am indebted to Professor Geoffrey F. Chew, Professor Arthur H. Rosenfeld, and Professor M. Lynn Stevenson for their most appreciated advice and criticism. I wish especially to thank my co-workers on this experiment, Jerry Anderson, Dr. Phillip G. Burke, Dr. Norbert Schmitz, and Dr. Remy van de Walle.

This experiment would not have been possible without the aid of the Bevatron and Bubble Chamber crews.

I wish to thank the physicists, grad students and "beam watchers" (especially Jack Lloyd) who labored on the beam. I am grateful to Dave Johnson for his help on the use of the EXAM system. I am further grateful to all of the scanners who have worked on this experiment.

This work was done under the auspices of the U. S. Atomic Energy Commission.

APPENDICES

A. Beam Momentum, Path Length, Scanning Efficiency, and Beam Contamination

1. Beam Momentum

The large size of the 72-inch chamber was efficiently used by Professor Frank Crawford to provide an over-all calibration of the film taken during the run for the associated-production study. The threshold of the reaction

$$\pi^- + p \rightarrow \Sigma^- + k^+ \tag{A-1}$$

was placed in the chamber and (s-wave) threshold rise as a function of position in the chamber was observed.[19] It was then possible to unfold the position of threshold in the chamber. By use of PANG, the momentum was measured for a number of beam tracks and the momentum from curvature as compared to the momentum at threshold was calculated from the known masses. It was thus found that our PANG needed to be corrected by $1.0065 \pm .005$.[20] In order to calibrate the portion of the film used in this experiment, PANG was used to measure curvature and this correction was applied. Subsequent measurements of the magnetic field of the 72-inch bubble chamber have indicated that it did indeed need to be modified by about 0.5% in the direction indicated by our calibration.

The momentum of the π^+ beam was found to be 1255 ± 6 Mev/c. The π^- beam included two momenta, 1252 ± 6 Mev/c and 1282 ± 6 Mev/c.

The errors above are statistical. The actual width of the beam used is ± 16 Mev/c, where the width comes mostly from the thickness of the chamber (the length of the fiducial volume is 60 inches).

2. Path Length and Scanning Efficiency

In order to establish the path length scanned, the scanners counted beam tracks on every twentieth frame simultaneous with and using the same criteria as used in the scan. The π^- film was scanned once (except for 10% of it, which was scanned twice). The π^+ film was double-scanned. The scanning efficiency of each scanner was determined and the over-all π^- and π^+ scanning efficiencies were found by averaging each scanner's efficiency weighted by the amount of film he scanned. The π^- efficiency was 83%. The π^+ first-scan efficiency was 87%, the second 85%, leading to a combined efficiency of 98% (under the assumption of no correlation between scans: $e_{12} = e_1 + e_2 - e_1 e_2$). The path length was corrected for unmeasurable events, and, since the track counting was done with the same criteria as the scanning, the path length was corrected by the small fraction of events that did not have the beam momentum within 50 Mev/c of nominal. The corrected path lengths are $L_- = 4.73 \times 10^7$ cm and $L_+ = 4.17 \times 10^7$ cm.

3. Beam Contamination

The above path lengths have also been corrected for the beam contamination. The π^- beam was corrected for a 3% contamination by leptons and the π^+ beam was corrected for a 3% contamination by leptons and a 2% contamination by protons. The leptonic contamination was found by Leroy Price and Jerry Meissner (Lawrence Radiation Laboratory) by counting large delta rays. (For details of the determination of the proton contamination see Ref. 20.) It was found that when the film was scanned at grazing incidence, the less "gappy" protons appear to be solid tracks, whereas the pions remain "gappy." Furthermore, a typical proton has 20-minute delta rays per chamber length and a pion has 12. Neither of these methods is easily applied to a contamination as low as 2% because there is some variation in ionization from frame to frame. This difficulty was overcome by determining the fraction of protons in the chamber as a function of the height of the beam profile (the pion and proton image was separated by an electrostatic separator and the height of the image was then controlled by variation of a crossed magnetic field). We could then extrapolate to the actual operating condition.

B. Chew-Low Method

In order to derive the expression given here as Eq. (II-11), Chew and Low have made the following three conjectures.[13]

1. Consider the process $\pi + p \rightarrow p + \pi + \pi^0$ (see Fig. 4a). Because there exists a single-particle state (π^0) which can connect the left- and right-hand sides of Fig. 4a, it is conjectured that the scattering amplitude

expressed as a function of the four-momentum of either the left- or right-hand side of Fig. 4a has a pole at the mass of the intermediate particle.

2. It is conjectured that the scattering amplitude for the process $\pi + p \rightarrow p + \pi + \pi^0$ becomes equal to the $p \rightarrow p + \pi^0$ vertex function times the vertex function times the π^0 propagator when the π^0 is on its mass shell.

3. It is further conjectured that the scattering amplitude of the right-hand side of Fig. 4a evaluated with the intermediate π^0 on its mass shell is the physical matrix element for the real process $\pi + \pi^0 \rightarrow \pi + \pi^0$.

The cross section for the process $\pi + \pi^0 \rightarrow \pi + \pi^0$ can be written

$$\sigma_{\pi\pi}(\omega^2) = \frac{2\pi}{P'_{in}} \left| \left\langle \omega^2 \middle| j \middle| P_{in} \right\rangle \right|^2 , \tag{B-1}$$

where P'_{in} is the flux factor in the system where the π^0 is at rest. P'_{in} can be expressed in terms of the total di-pion mass, ω^2, by

$$\left(\sqrt{P'^2_{in} + 1} + 1\right) - P'^2_{in} = \omega^2 - 0^2 , \tag{B-2}$$

$$P'_{in} = \sqrt{\omega^2\left[\omega^2/4-1\right)} . \tag{B-3}$$

(see Equations II-6 through II-10 for definition).

The matrix element for the process $p \rightarrow p + \pi$ is $4\pi f^2 p^2$, where f is the renormalized pion-nucleon coupling constant.

Thus the cross section for the process $\pi + p \rightarrow p + \pi + \pi^0$ at $p^2 = -1$ is, by our conjectures,

$$\frac{\Delta\sigma_{\pi p}}{\Delta\tau} = \frac{2\pi}{P_{in}} \int_\tau \frac{4\pi f^2 p^2}{(p^2+1)^2} \left| \left\langle \omega^2 \middle| j \middle| P_{in} \right\rangle \right|^2 4M\,\delta(Q'^2+M^2) \frac{d^4Q'^2}{(2\pi)^3} , \tag{B-4}$$

where Q' is the four-momentum of the recoil proton, that is $p^2 = (Q-Q')^2$, where Q is the four-momentum of the incident proton. But we have

$$\int d^4 Q' \,\delta\,(Q'^2 + M^2) = \frac{P_p 2\pi \, d(\cos\Theta_p)\, dE_p}{2}, \tag{B-5}$$

and making a transformation of variables by using Eq. (II-6) and (II-7), we obtain

$$\int d^4 Q' \,\delta\,(Q'^2 + M^2) = \frac{\pi}{4MP_{in}}\, dp^2\, d\omega^2. \tag{B-6}$$

Thus

$$\lim_{p^2 = -1} \frac{d^2\sigma_{\pi p}}{dp^2 d\omega^2} = \frac{f^2 \sqrt{\omega^2[\omega^2/4]-1)}}{2\pi P_{in}^2} \frac{p^2}{(p^2+1)^2}\, \sigma_{\pi\pi}(\omega^2), \tag{B-7}$$

which is Eq. (II-11).

C. Extension of the Chew-Low Method to Measurement of the Differential Pion-Pion Interaction

In order to carry out an extrapolation to the differential pion-pion cross section, one must know the analytic structure of the amplitude $A_{\pi p}(p^2, \omega^2, q_\pi q_\pi')$ as a function of p^2 for fixed ω^2 and fixed $q_\pi q_\pi'$.[14] Recall (see Chapter II, Section D)

$$q_\pi q_\pi' = p_\pi p_\pi' \cos\theta_{\hat{\pi}\hat{\pi}} - \epsilon_\pi \epsilon_\pi', \tag{C-1}$$

where

$$\epsilon_\pi = \frac{\omega^2 + p^2 + 1}{2\omega} \qquad \epsilon_\pi' = \omega/2, \tag{C-2}$$

and

$$p_\pi = \sqrt{\frac{(\omega^2+p^2+1)^2}{(2\omega)^2} - 1}\;\; \frac{1}{2\omega}\sqrt{[p^2+(\omega+1)^2][p^2+(\omega-1)^2]},$$

$$p_\pi' = \sqrt{[\omega^2/4]-1}\;. \tag{C-3}$$

Thus

$$q_\pi q'_\pi = \frac{\omega^2+p^2+1}{4} - \frac{\sqrt{(\omega^2/4)-1}}{2\omega}\sqrt{[p^2+(\omega+1)^2][p^2+)\omega-1)^2]} \ . \qquad \text{(C-4)}$$

We see that the invariant $q_\pi q'_\pi$ has branch points at $p^2 = -(\omega+1)^2$ and $p^2 = -(\omega-1)^2$. The analytic structure of $A_{\pi p}$ is therefore as given in Fig. 5b. We note that for $\omega^2 = 16$, the additional branch cut runs from -9 to -25, that is, it lies on the already existing branch cut. We have therefore assumed that for $\omega^2 > 16$ we can use the fitting procedure of Eq. (II-11) to evaluate the differential pion-pion cross section. That is,

$$(p^2+1)^2\, d^3\sigma/dp^2 d\omega^2 d\cos\theta_{\pi\pi} = A'_0 + A'_1(p^2+1) + A'_2(p^2+1)^2 + \cdots , \qquad \text{(C-5)}$$

and therefore

$$d\sigma_{\pi\pi}(\omega^2)/d\cos\theta_{\pi\pi} = -A'(\omega^2)\ \frac{2\pi}{f^2}\ p_{in}^2\ \omega[\omega^2/4]-1)^{1/2} \ .$$

D. Isotopic Spin and the Role it Plays in the Angular Momentum Decomposition

The differential cross section for the process $\pi^+ + \pi^0 \rightarrow \pi^+ + \pi^0$ can be written

$$d\sigma_{\pi\pi}/d\cos\theta_{\pi\pi} = 2\pi\lambda^2 \,|\, A_{\pi\pi^0\rightarrow\pi\pi^0}(\omega^2, \cos\theta_{\pi\pi})|^2 , \qquad \text{(D-1)}$$

where

$$A(\omega^2, \cos\theta_{\pi\pi}) = \sum_\ell (2\ell+1)\, A_\ell(\omega^2)\, P_\ell(\cos\theta_{\pi\pi}) \qquad \text{(D-2)}$$

and

$$A_\ell(\omega^2) = e^{i\delta_\ell} \sin\delta_\ell \ . \qquad \text{(D-3)}$$

The amplitude $A_{\pi\pi\rightarrow\pi\pi}$ can be expanded in terms of isotopic spin and amplitudes:

$$A_{\pi^+\pi^0\rightarrow\pi^+\pi^0} = \frac{1}{2}\, A^1 + \frac{1}{2}\, A^2 \ . \qquad \text{(D-4)}$$

The generalized Pauli Principle in the case of spinless bosons requires that the T-spin function and the space wave function be even. The T=2 T-spin states are even (and the T=2 T-spin states are odd) under interchange of the two pions. The Legendre polynomials have the parity $(-1)^{\ell}$.
Thus

$$A^{'}(\omega^2, \cos\theta_{\pi\pi}) = \sum_{\text{odd}\,\ell} (2\ell+1)\, A_\ell(\omega^2)\, P_\ell(\cos\theta_{\pi\pi}), \tag{D-5}$$

$$A^2(\omega^2, \cos\theta_{\pi\pi}) = \sum_{\text{even}\,\ell} (2\ell+1)\, A_\ell(\omega^2)\, P_\ell(\cos\theta_{\pi\pi}). \tag{D-6}$$

We shall therefore denote the phase shifts, δ_ℓ^I, of the reaction $\pi^+ + \pi^0 \to \pi^+ + \pi^0$ as δ_0^2, $\delta_1^{'}$, δ_2^2, and $\delta_3^{'}$ $\cdots$.
Two remarks about the phase shifts should be made concerning a resonance at $\omega^2 = 29$. 1. The phase shifts need not be real. 2. The c.m. wave number of the pions is 2.5 pion Compton wave lengths. Thus d or f waves may be present.
Under the assumption of (real) s and p waves only, however, Eqs. (AIV-1), (AIV-2), and (AIV-3) yield

$$d\sigma_{\pi^+\pi^0}/d\cos\theta_{\pi\pi} \tag{D-7}$$

$$= 2\pi\lambda\!\!\!^{-2}[\sin^2\delta_0 + 6\sin\delta_1\sin\delta_0\cos(\delta_1-\delta_0)\cos\theta_{\pi\pi} + 9\sin^2\delta_1\cos^2\theta_{\pi\pi}],$$

and under the assumption of a pure p state,

$$d\sigma_{\pi^+\pi^0}/d\cos\theta_{\pi\pi} = 18\pi\lambda\!\!\!^{-2}\sin^2\delta_1\cos^2\theta_{\pi\pi}, \tag{D-8}$$

thus the total cross section for a p-state resonance is

$$\sigma_{\pi^+\pi^0} = 12\pi\lambda\!\!\!^{-2} = 12\pi/(\omega^2/4-1). \tag{D-9}$$

E. Combining Unlike Data before Extrapolation

Case 1. Same beam momenta but unlike charge states

Consider the reactions $\pi^- + p \to p + \pi^- + \pi^0$ and $\pi^+ + p \to p + \pi^+ + \pi^0$ at the same beam momentum. By charge independence, we know that the extrapolation of either reaction leads to the same pion-pion cross section (same residue of the pole in the scattering amplitude). Because of the difference of charge combinations in the final-state interactions between the proton and one of the pions (see Fig. 4c), we do not expect equal contributions to the branch cut in both reactions.

Nevertheless, we can combine the two reaction before extrapolation. Let $N_+(p^2)$ be the number of events found in the π^+ film in a path length L_+. Let $N_-(p^2)$ be the number of events found in the π^- film in a path length L_-. Let $N(p^2) = N_+(p^2) + N_-(p^2)$. Then, by Eqs. (II-11) and (II-17) we have

$$\sigma_{\pi^-\pi^0} \propto \frac{N_-(p^2=-1)}{L_-} , \quad \sigma_{\pi^+\pi^0} \propto \frac{N_+(p^2=-1)}{L_+} , \tag{E-1}$$

but, by hypothesis, $\sigma_{\pi^+\pi^0} = \sigma_{\pi^+\pi^0}$. Define an effective path length for the combined experiment, L. Then

$$L \propto \frac{N}{\sigma_{\pi\pi^0}} = \frac{N_+}{\sigma_{\pi^+\pi^0}} + \frac{N_-}{\sigma_{\pi^-\pi^0}} = L_+ + L_- \tag{E-2}$$

That is, $N = N_+ + N_-$ and $L_+ L_-$.

Case 2. Different beam momenta

As discussed in Appendix A, the π^- film was found to consist of two beam momenta, namely 1255 Mev/c and 1282 Mev/c. These two momenta were combined before extrapolation according to the following considerations (see Eq. II-11):

$$\sigma_{\pi\pi}(\omega^2) \propto \frac{1}{\left(\frac{L}{P_{in}^2}\right)} \lim_{p^2 \to -1} (p^2+1)^2 \frac{N'(p^2,\omega^2)}{\Delta p^2 \Delta\omega^2} . \tag{E-3}$$

Thus the effect of the slight variation of P_{in} can be compensated for by modifying the path length of one of the momenta by the square of the ratio of the momenta and by correcting each momentum according to its own phase space Δp^2 $\Delta\omega^2$)see Fig. 6).

References

1. Jerry A. Anderson, Phillip G. Burke, D. Duane Carmony, and Norbert Schmitz, in Proceedings of the 1960 Annual International Conference on High Energy Physics at Rochester (Interscience) p. 58.
2. Jerry A. Anderson, V. O. X. Bang, Phillip G. Burke, D. Duane Carmony, and Norbert Schmitz, Phys. Rev. Letters 6, 365 (1961).
3. Jerry A. Anderson, V. O. X. Bang, Phillip G. Burke, D. Duane Carmony, and Norbert Schmitz, Revs. Modern Phys. 33, 431 (1961).
4. I. Derado and Norbert Schmitz, Phys. Rev. 118, 309 (1960).
5. Gerald Lynch, Alvarez Group Memo 135.
6. For a description of PANG, see William E. Humphrey, Alvarez Group Memo 111.
7. For a description of KICK, see Arthur H. Rosenfeld, Reference Manual for KICK, UCRL-9099, May 1961.
8. For a description of EXAM, see David Johnson, Alvarez Group Memo 271, and Remy van de Walle and D. Duane Carmony, Alvarez Group Memo 352.
9. Norbert Schmitz, Alvarez Group Memo 211.
10. Alan Natapoff, Alvarez Group Memo 277.
11. William R. Frazer and Jose R. Fulco, Phys. Rev. 117, 1609 (1960).
12. F. J. Bowcock, W. N. Cottingham, and D. Lurie, Phys. Rev. Letters 5, 386 (1960).
13. Geoffrey F. Chew and F. E. Low, Phys. Rev. 113, 1640 (1959).
14. Michael Nauenberg, Phys. Rev. Letters 5, 438 (1960).
15. D. Duane Carmony and Remy van de Walle, Total and Differential π-π Cross Sections in π-p Interactions at 1.25 Bev/c (submitted to Phys. Rev. Letters) and D. Duane Carmony and Remy van de Walle, The π-π Cross Section – An Application of the Chew-Low Extrapolation Procedure, UCRL-9933 (1961), submitted to Phys. Rev., also contain a discussion of the results of this experiment.

16. G. A. Smith, H. Courant, E. Fowler, H. Kraybill, J. Sandweiss, and H. Taft, Phys. Rev. Letters 5, 571 (1960).

17. This is in agreement with the results of Janos Kirz, Joseph Schwartz and Robert Trip (To be submitted to Phys. Rev. Letters). They have shown that the s-wave interaction is small at zero energy.

18. A. R. Erwin, R. March, W. D. Walker, and E. West, Phys. Rev. Letters 6, 628 (1961).
E. Pickup, D. K. Robinson, and E. O. Salant, Phys. Rev. Letters 7, 192 (1961).

19. Margaret H. Alston, Jerry A. Anderson, Phillip G. Burke, D. Duane Carmony, Frank S. Crawford, Jr., Norbert Schmitz, and Sanford E. Wolf, in Proceedings of the 1960 Annual International Conference on High Energy Physics at Rochester (Interscience) p. 377.

20. Remy van de Walle and D. Duane Carmony, Alvarez Group Memo 351.